

DYNAMICS OF A LIQUID HELIUM I CRYOSTAT AT THE CANADIAN LIGHT SOURCE

C. Regier¹

¹Canadian Light Source Inc.
Saskatoon, SK, S7N 0X4, Canada.

ABSTRACT

The Canadian Light Source (CLS) is a third-generation synchrotron located in Saskatoon, Canada. A superconducting radio frequency (SRF) cavity contained in a 4.43 K liquid helium I cryostat is used at the CLS to replenish energy loss in the electron beam. A dynamic simulation of this cryostat has been generated to examine pressure and level fluctuations due to variations in heat loading or other system parameters. This simulator has led to some interesting observations in system behavior, which have been shown to occur in the actual system as well. For example, mass rates of vaporization appear to drop as heat loading increases under certain conditions. Also, the relationship between pressure and SRF tuning characteristics is examined, and the abilities and limitations of the simulator are presented.

KEYWORDS: Cryostat, Helium I, Process Control

INTRODUCTION

The Canadian Light Source (CLS) is a 3rd generation synchrotron facility located in Saskatoon, Canada. At the CLS electrons are accelerated to virtually the speed of light through a linear accelerator and booster ring, and then injected into a storage ring where this velocity is maintained. Magnets are used to steer the electron beam, and at various points undulators and wigglers are used to cause the beam to oscillate as it moves through the storage ring. As the electron beam is steered and oscillated, it gives off very intense radiation covering most of the electromagnetic spectrum. This “light” is siphoned off of the storage ring and is used in experimental research into such topics as nanotechnology, semiconductor behavior, pharmaceuticals, materials science, and medical imaging.

The emission of this “synchrotron light” causes a loss in momentum in the electron beam, which is compensated for using a superconducting radio frequency (SRF) cavity in

one portion of the storage ring. This SRF cavity is constructed from niobium, and is kept in a liquid helium (LHe) bath at 4.4 K to maintain superconductivity. The cryostat containing the cavity is therefore at boiling equilibrium, and the equilibrium point is shifted when cryostat conditions, such as pressure or liquid level, are varied.

Due to the sometimes counterintuitive nature of boiling two-phase systems, the controls group at the CLS can benefit from a simulator that can approximate the behavior of the cryogenic system, including the cryostat containing the SRF cavity. To this end, a simulation of part of the system, including the LHe transfer line, cryostat, and cold gas return system, has been constructed. The LHe transfer line modeling is described in [1], while the cryostat model, around which this work is based, is covered in [2].

This paper begins with a brief discussion of the CLS cryogenic system, as well as some background on the SRF cryostat itself. The mathematical model of the cryostat used for the following work is briefly presented, though for the details in the model the reader is referred to [2]. In using the cryostat model discussed in [2], the author has observed some interesting simulator output that is sometimes counterintuitive, and these behaviors are presented here. Experimental data is used to verify simulator output where possible, however limited instrumentation in the actual cryostat means that some data were generated using values calculated based on the experimental results. For example, the boiling rate in the cryostat cannot be directly measured and must be inferred based on other system data such as level, pressure, and cold helium gas return flow which can be directly measured.

THE CLS CRYOGENIC SYSTEM

The LHe cryogenic system at the CLS is shown in FIGURE 1. The design load for the system is 284 W. A compressor takes warm helium gas from near atmospheric pressure and compresses it to 10 bar. The warm gas is then passed through a series of heat exchangers, which exchange heat with the cold return gas from the system, and turbines, which reduce the enthalpy of the helium by using it to do work. A Joule-Thompson valve partially liquefies the cooled helium gas, and the liquid is deposited in a 2000 L dewar.

A pressure differential of 0.15 bar is used to drive the liquid from the dewar through a 60 m long vacuum-jacketed transfer line to the cryostat. A level control valve on the transfer line regulates liquid flow to maintain a constant liquid level in the cryostat. A similar control valve on the cold gas return line regulates cryostat pressure and allows the cold gas to return to the cryogenic plant, where it is passed through the heat exchangers, warmed to room temperature, and fed back to the compressor inlet.

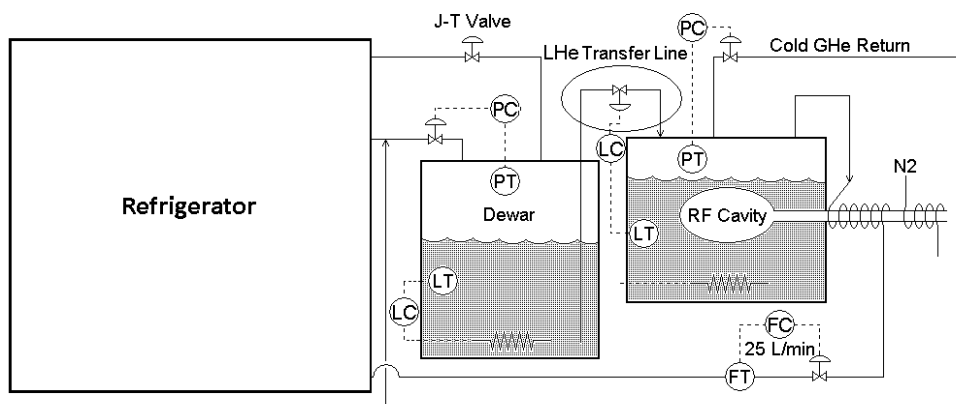


FIGURE 1. A schematic of the CLS SRF Cryogenic System.

The SRF cryostat is depicted in FIGURE 2. This cryostat has a total helium volume of 502 L after taking into account the fluid displaced by the SRF cavity and other internal objects. There is a heater on the bottom of the cryostat which allows a load to be placed on the system even when the radio frequency (RF) system is not operating. This heater is also used as a load leveler for the RF, meaning that if the RF fluctuates the heater will fluctuate in an equal and opposite way to maintain a constant load on the system. Due to internal obstructions, the level meter is set in the cryostat in such a way that there is a significant difference between indicated and actual level. Typical operating points are 1220 mbar pressure and 493 L of liquid in the cryostat, which equates to an actual level of around 94%, but an indicated level of 75%. Indicated values are used throughout this paper.

THE CRYOSTAT MODEL

The model used to evaluate the SRF cryostat is described in detail in [2] and is heavily based on a model of a vessel containing a boiling liquid given in [3]. This model is based on mass balances of gas and liquid in the cryostat, the energy balance, the relationship between the boiling temperature and pressure of a pure substance, and the real gas law. These relationships are used to formulate the expression for the boiling rate of the helium given in equation (1).

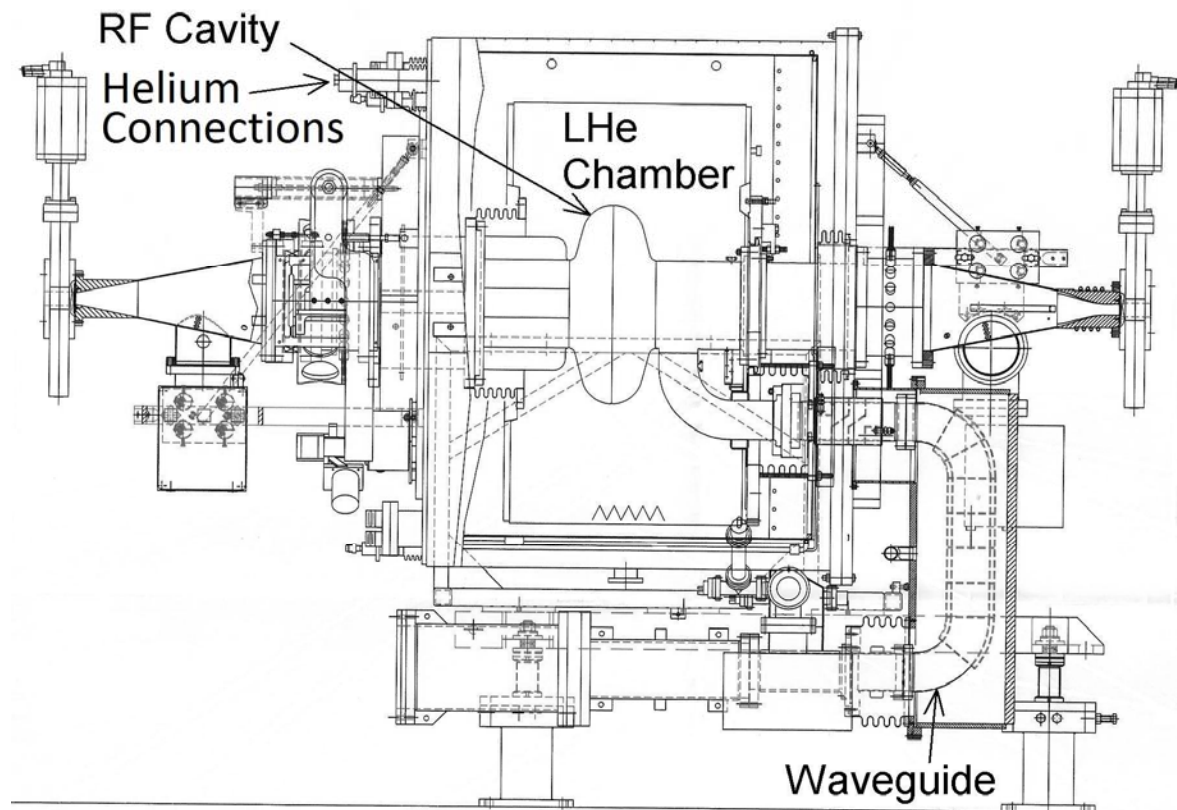


FIGURE 2. The SRF cryostat at the CLS, showing the SRF cavity in the middle, along with the RF waveguide leading into the cryostat from the amplifier.

$$\dot{m}_{Boil} = \frac{-\frac{a_1}{a_2} (a_3 + 0.0585 a_4 m_L \phi P^{-0.748}) + a_4 \left(\frac{V_G}{m_G} (\dot{m}_{Gout} - \dot{m}_{Gin}) + a_5 (\dot{m}_{Lout} - \dot{m}_{Lin}) \right)}{\frac{u_L - u_G}{a_2} (a_3 + 0.0585 a_4 m_L \phi P^{-0.748}) + a_4 \left(\frac{V_G}{m_G} - a_5 \right)} \quad (1)$$

where m_L is the mass of liquid in the cryostat in kg, ϕ is the rate of change of liquid specific volume with temperature in $\text{m}^3/\text{kg-K}$, P is the cryostat gas pressure in Pa, V_G is the total gas volume in the cryostat in m^3 , m_G is the mass of gas in the cryostat in kg, \dot{m}_{Gout} is the mass flow rate of gas out of the cryostat in kg/s, \dot{m}_{Gin} is the mass flow rate of gas into the cryostat in kg/s, \dot{m}_{Lout} is the mass flow rate of liquid out of the cryostat in kg/s, \dot{m}_{Lin} is the mass flow of liquid into the cryostat in kg/s, u_L is the specific internal energy of the liquid in the cryostat in J/kg, and u_G is the specific internal energy of the gas in the cryostat in J/kg. The terms a_1 through a_5 are simplification terms and are defined by equations (2) through (6) as

$$a_1 = \dot{Q} + \dot{m}_{Lin} (h_{Lin} - u_{Lin}) + \dot{m}_{Gin} (h_{Gin} - u_{Gin}) - \dot{m}_{Lout} (h_L - u_L) - \dot{m}_{Gout} (h_G - u_G) \quad (2)$$

where \dot{Q} is heat transfer into the cryostat fluid from all sources in W, h_{Lin} is the specific enthalpy of the incoming liquid in J/kg, u_{Lin} is the specific internal energy of the incoming liquid in J/kg, h_{Gin} is the specific enthalpy of the incoming gas in J/kg, u_{Gin} is the specific internal energy of the incoming gas in J/kg, h_L is the specific enthalpy of the liquid in the cryostat in J/kg, and h_G is the specific enthalpy of the gas in the cryostat in J/kg,

$$a_2 = m_L \frac{du_L}{dP} + m_G \frac{du_G}{dP} \quad (3)$$

$$a_3 = \left(0.0585 P^{-0.748} - \frac{(16.444 \times 10^{-6} P + 0.4967) V_G}{R m_G} \right) \quad (4)$$

where R is the specific gas constant for helium, 2077.15 J/kg-K,

$$a_4 = \frac{(8.222 \times 10^{-6} P^2 + 0.4967 P)}{R m_G} \quad (5)$$

and

$$a_5 = 0.232 \phi P^{0.252} + \varphi \quad (6)$$

where φ is a constant and equal to 0.0004873. The terms ϕ and φ come from the relationship between liquid specific volume and temperature, and for this work $\phi = 0.0017612$ and $\varphi = 0.0004873$ describes this relationship based on NIST data [4] to within +/- 0.5%.

The model was validated by comparing model response to the actual system response to various conditions, including cryostat fill rate and the cold gas outflow rate for various cryostat heater outputs. The results are shown in FIGURE 3, and indicate a good match between model and physical system.

RESULTS AND OBSERVATIONS

Pressure Transients due to Heat Loading

During discussions at the CLS, it was mentioned that reducing the normal operating liquid level in the cryostat might result in cryostat pressure being more robust to variations in heat loading. This might then result in a lower peak pressure seen in the cryostat when heat spikes in the SRF cavity occur, which in turn might result in better RF phase tuning for the beam. The theory behind this is that a larger gas volume in the top of the cryostat might act as a spring to absorb pressure fluctuations.

The simulator, however, indicates that this is not the case, and in fact in simulations the peak pressure actually decreased slightly for higher liquid levels. While peak pressure was not improved by reducing liquid level, the simulator showed that it could potentially be improved by increasing pressure gain. These results are shown in FIGURE 4.

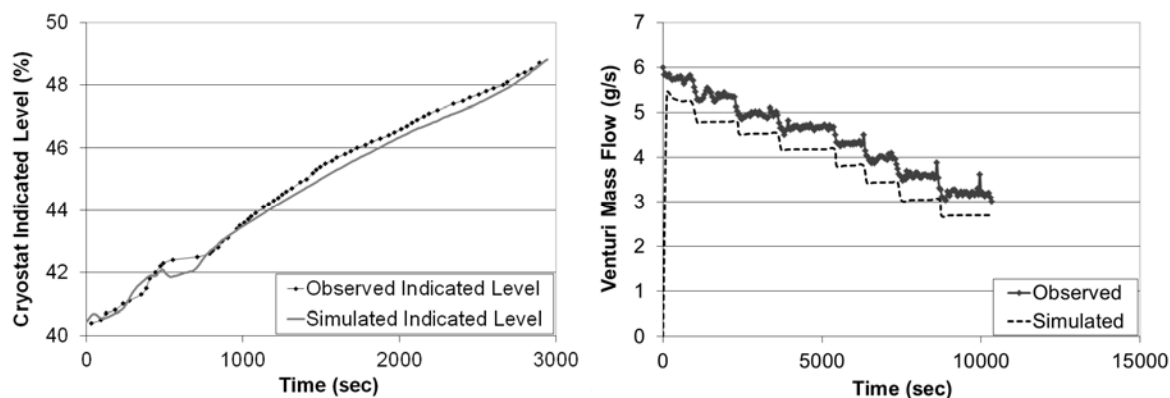


FIGURE 3. Simulated and actual results for cryostat filling (left) and cold gas return mass flows for various cryostat heater power settings (right). For the plot on the right heater settings are reduced in approximately 10 W steps over time from a high point of 70 W to a low point of 0 W, and the flows are measured using a venturi located on the cold gas return line about 3 m from the cryostat.

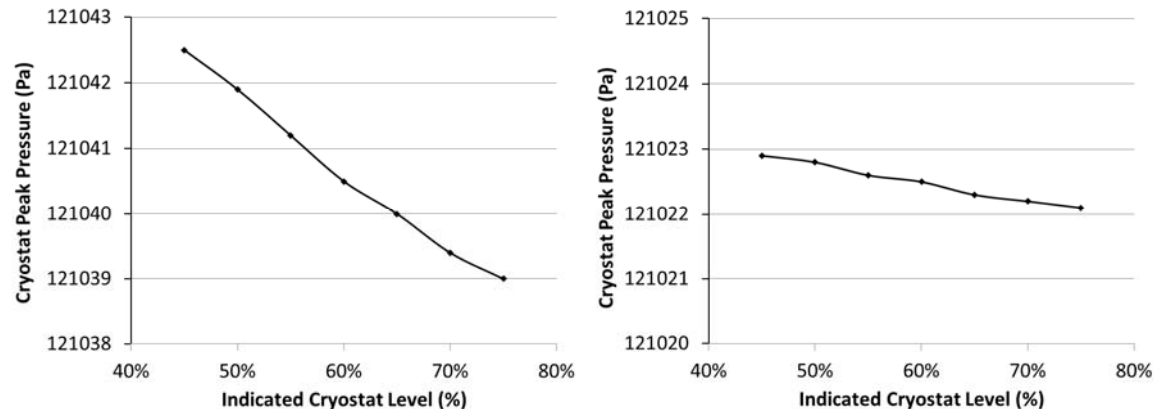


FIGURE 4. Maximum spike in cryostat pressure for a 30 W jump in heat load using standard pressure PID controller gains (left) and with pressure control gains multiplied by 10 (right).

Boil Rate Reduction for Increased Heat Loading

While examining simulator results, an interesting and counterintuitive phenomenon was observed. For high cryostat liquid levels the boil rate dropped when the heater power output was increased. FIGURE 5 shows simulator boil rate output for a 30 W heat increase at time $t=0$ when the cryostat is filled to an indicated level of 50% which equates to an actual level of 65%, while FIGURE 6 shows the same data when the cryostat is filled to an indicated level of 75%, which equates to an actual level of 94%. FIGURE 7 demonstrates the relationship between indicated level and boil rate, as well as between liquid volume in the cryostat and boil rate.

This effect has been discussed with multi-phase researchers and other scientists using the same cryostat and SRF design, and no satisfactory explanation has yet been offered. The model mathematics have been examined exhaustively, and potential effects of nonlinearities in linear approximations used in the model have been looked at as well. None of this has yielded answers as to the observed simulator behavior seen in FIGURES 5 and 6.

While the CLS cryostat does not have instrumentation available to directly measure the boil rate, a boil rate in the actual cryostat can be calculated based on the measured level and pressure using NIST data [4]. This was done for similar conditions to those used in the simulator and the results are compared with simulator data in TABLE 1.

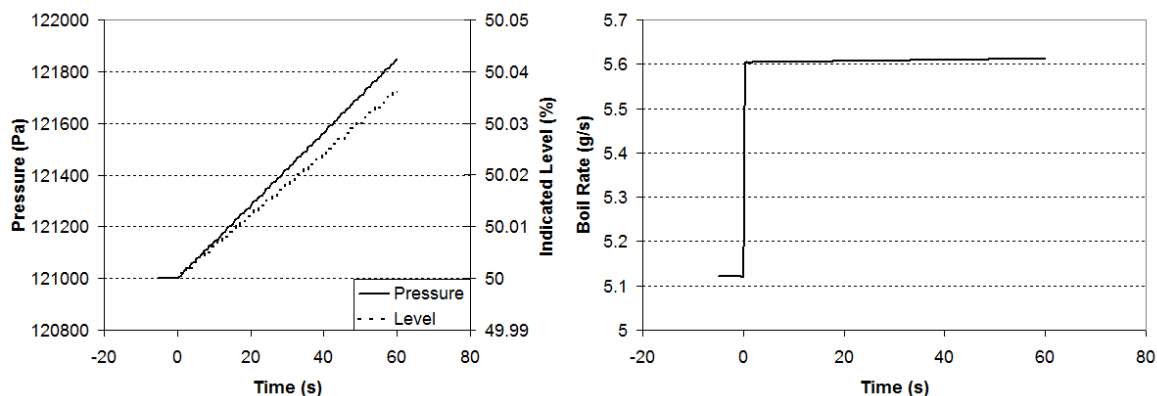


FIGURE 5. Simulated mass rate of boiling for the cryostat with a 30 W heat increase applied at time $t=0$ for a 50% indicated level.

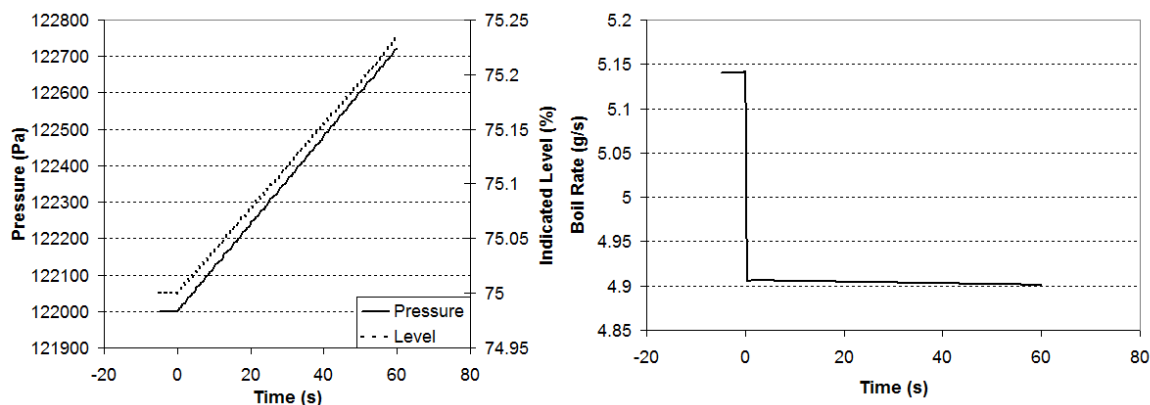


FIGURE 6. Simulated mass rate of boiling for the cryostat with a 30 W heat increase applied at time $t=0$ for a 75% indicated level.

TABLE 1. Boil rates calculated based on measured level and pressure data in the cryostat for three trials at 75% indicated level and one trial at 50% indicated level.

	Trial	Boil Rate Change (g/s)
Measured	1 - 75% Level	-0.379
	2 - 75% Level	-0.367
	3 - 75% Level	-0.389
	4 - 50% Level	0.786
Simulated	75% Level	-0.271
	50% Level	0.486

While not a perfect match, the experimental values in TABLE 1 do appear to be reasonably close to the simulated values, and more importantly demonstrate that the phenomenon of boil rate drop at high levels was also observed experimentally. It should be noted, however, that the level increments used to collect this data were quite small, and that the level indicator on the SRF cryostat outputs a somewhat noisy signal. Therefore, while the data support the simulator output, it is not possible to state conclusively from this information that the boil rate drops with increased heat loading in the actual system. Further testing is in progress to verify these results.

CONCLUSION

This work used an existing computer simulator for the SRF LHe cryostat at the CLS to examine properties of the cryostat and its behavior. The simulator indicated that increasing the volume of gas in the cryostat by reducing liquid level would not help moderate pressure spikes due to disturbance heat loading in the cryostat, but that increasing pressure controller gains could. When the liquid level was high, a decrease in the simulated boil rate was observed for an increase in heat load. This effect was duplicated, with some uncertainty, on the actual system, but no physical explanation yet exists for this behavior.

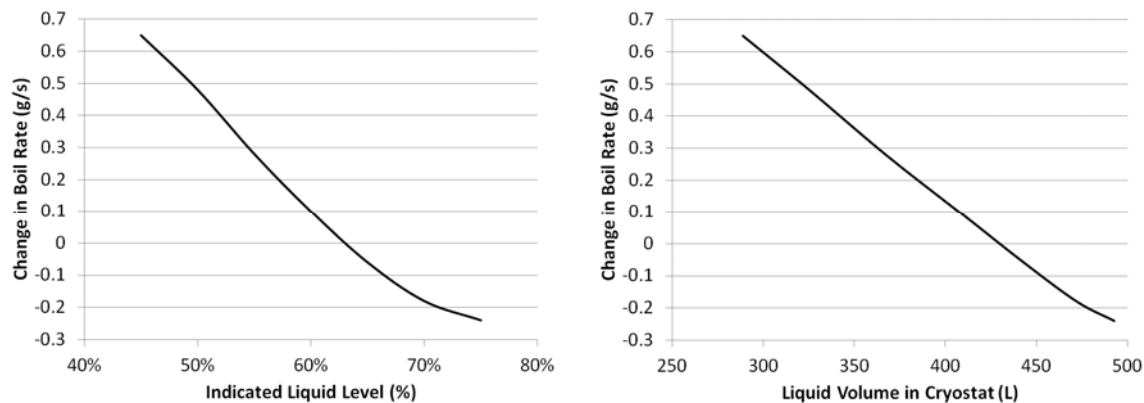


FIGURE 7. The simulated change in mass rate of boiling for a heat increase of 30 W in the cryostat based on indicated level (left) and liquid volume in the cryostat (right).

ACKNOWLEDGEMENTS

The author wishes to acknowledge the following individuals for their assistance in this work: Jeff Pieper and Elder Matias for their contributions to creating the cryostat model, Jon Stampe and Carl Jansen for their help with operating the cryogenic system, and their ideas on system performance, Mark de Jong, Abdulmajeed Mohamad, Jim Bugg, and Carey Simonson for their expertise in cryogenics, fluid mechanics, and heat transfer, and Michael Pekeler for his assistance in determining various system parameters.

REFERENCES

1. Regier, C., Pieper, J., and Matias, E., *Cryogenics* **51**, pp. 1-15 (2011).
2. Regier, C., Pieper, J., and Matias, E., *Cryogenics* **50**, pp. 118-125 (2010).
3. Thomas, P., *Simulation of Industrial Processes for Control Engineers*, Butterworth-Heinemann, Linacre House, Jordan Hill, Oxford, 2002.
4. Lemmon, E., McLinden, M., and Friend, D., "Thermophysical Properties of Fluid Systems," in *NIST Chemistry Webbook, NIST Standard Reference Database Number 69*, edited by P. Linstrom and W. Mallard, National Institute of Standards and Technology, Gaithersburg, MD, 2008. Accessed from <http://webbook.nist.gov/chemistry/fluid>, date accessed, June 9, 2008.